



## Evaluation of the Alphasense optical particle counter (OPC-N2) and the Grimm portable aerosol spectrometer (PAS-1.108)

Sinan Sousan, Kirsten Koehler, Laura Hallett & Thomas M. Peters

**To cite this article:** Sinan Sousan, Kirsten Koehler, Laura Hallett & Thomas M. Peters (2016) Evaluation of the Alphasense optical particle counter (OPC-N2) and the Grimm portable aerosol spectrometer (PAS-1.108), *Aerosol Science and Technology*, 50:12, 1352-1365, DOI: [10.1080/02786826.2016.1232859](https://doi.org/10.1080/02786826.2016.1232859)

**To link to this article:** <http://dx.doi.org/10.1080/02786826.2016.1232859>



[View supplementary material](#)



Accepted author version posted online: 07 Sep 2016.  
Published online: 07 Sep 2016.



[Submit your article to this journal](#)



Article views: 678



[View related articles](#)



[View Crossmark data](#)



Citing articles: 4 [View citing articles](#)

Full Terms & Conditions of access and use can be found at  
<http://www.tandfonline.com/action/journalInformation?journalCode=uast20>

## Evaluation of the Alphasense optical particle counter (OPC-N2) and the Grimm portable aerosol spectrometer (PAS-1.108)

Sinan Sousan<sup>a</sup>, Kirsten Koehler<sup>b</sup>, Laura Hallett<sup>a</sup>, and Thomas M. Peters  <sup>a</sup>

<sup>a</sup>Department of Occupational and Environmental Health, University of Iowa, Iowa City, Iowa, USA; <sup>b</sup>Environmental Health Sciences, Johns Hopkins Bloomberg School of Public Health, Baltimore, Maryland, USA

### ABSTRACT

We compared the performance of a low-cost (~\$500), compact optical particle counter (OPC, OPC-N2, Alphasense) to another OPC (PAS-1.108, Grimm Technologies) and reference instruments. We measured the detection efficiency of the OPCs by size from 0.5 to 5  $\mu\text{m}$  for monodispersed, polystyrene latex (PSL) spheres. We then compared number and mass concentrations measured with the OPCs to those measured with reference instruments for three aerosols: salt, welding fume, and Arizona road dust. The OPC-N2 detection efficiency was similar to the PAS-1.108 for particles larger than 0.8  $\mu\text{m}$  (minimum of 79% at 1  $\mu\text{m}$  and maximum of 101% at 3  $\mu\text{m}$ ). For 0.5- $\mu\text{m}$  particles, the detection efficiency of the OPC-N2 was underestimated at 78%, whereas PAS-1.108 overestimated concentrations by 183%. The mass concentrations from the OPCs were linear ( $r \geq 0.97$ ) with those from the reference instruments for all aerosols, although the slope and intercept were different. The mass concentrations were overestimated for dust (OPC-N2, slope = 1.6; PAS-1.108, slope = 2.7) and underestimated for welding fume (OPC-N2, slope = 0.05; PAS-1.108, slope = 0.4). The coefficient of variation (CV, precision) for OPC-N2 for all experiments was between 4.2% and 16%. These findings suggest that, given site-specific calibrations, the OPC-N2 can provide number and mass concentrations similar to the PAS-1.108 for particles larger than 1  $\mu\text{m}$ .

### ARTICLE HISTORY

Received 9 June 2016  
Accepted 28 August 2016

### EDITOR

Jian Wang

## Introduction

Exposure to different size fractions of particulate matter (PM) has adverse health effects on human health in environmental and occupational settings (Antonini 2003; Bhatti et al. 2011; Landen et al. 2011; Polichetti et al. 2009; Samet and Krewski 2007). Particle deposition in the human respiratory tract and the consequent adverse health effects that may develop depends strongly on particle size (Brown et al. 2002; Schwartz and Neas 2000). Particle sizes of primary interest are particles smaller than 1  $\mu\text{m}$  (PM<sub>1</sub>, also known as submicron particles), particles smaller than 2.5  $\mu\text{m}$  (PM<sub>2.5</sub>, also known as fine particles), and particles smaller than 10  $\mu\text{m}$  (PM<sub>10</sub>). Exposures to different particle sizes have different effects on human morbidity and mortality. Increased mortality rates have been associated with PM<sub>2.5</sub> and PM<sub>10</sub> (Dockery et al. 1993; Landen et al. 2011; Ostro et al. 2015; Zanobetti and Schwartz 2009), lung cancer with PM<sub>2.5</sub> (Harrison et al. 2004; Pope et al. 2002), and cardiopulmonary diseases with PM<sub>1</sub>, PM<sub>2.5</sub>, and PM<sub>10</sub> (Burnett

et al. 1999; Franck et al. 2011; Järvelä et al. 2013; Ostro et al. 2015; Polichetti et al. 2009). Environmental studies show that PM<sub>2.5</sub> from combustion sources are more strongly associated with mortality (Schwartz et al. 1996) and adverse respiratory health effects (Schwartz and Neas 2000) than coarse particles (PM<sub>10-2.5</sub>).

A variety of methods are available to measure particle mass concentration. The Environmental Protection Agency (EPA) has established gravimetric filter reference methods to measure PM<sub>2.5</sub> and PM<sub>10</sub> for different particle sizes (EPA 1997a,b). Gravimetric filter methods are highly accurate and precise for providing particulate mass concentrations but do not provide temporal information. Cascade impactors use gravimetric and chemical analysis for mass determination and speciation at a wide range of particle sizes (Hinds 1999). Microscopy is a highly accurate method that uses optical methods for particles  $>0.3 \mu\text{m}$  and electron methods for small particles ( $<0.3 \mu\text{m}$ ) to determine particle size and shape (Hinds 1999), but can

**CONTACT** Thomas M. Peters  Thomas-m-peters@uiowa.edu  Department of Occupational and Environmental Health, University of Iowa, 105 River Street, S331 CPHB, Iowa City, IA 52242, USA.

Color versions of one or more of the figures in the article can be found online at [www.tandfonline.com/uast](http://www.tandfonline.com/uast).

 Supplemental data for this article can be accessed on the [publisher's website](#).

© 2016 American Association for Aerosol Research



have less precision for estimating mass concentrations. These methods are labor intensive, time-consuming, and expensive.

Various instruments enable automatic measurements of various size fractions of particulate mass concentrations indirectly using measurements of particulate number concentrations by size (Yanosky et al. 2002). A scanning mobility particle sizer (SMPS; cost: \$60,000+) is used to measure number concentration for submicron particles at different particle sizes (Knutson and Whitby 1975). The Aerodynamic Particle Scanner (APS 3321, TSI Inc., Shoreview, MN, USA; cost: \$45,000) is used to measure number concentration for large particle sizes, up to 20  $\mu\text{m}$ . Mass concentrations can be estimated from number concentrations by size measured with the SMPS and APS by making appropriate assumptions about particle density, although the large physical size and high cost of these instruments make them impractical for personal exposure assessment. Optical particle counters (OPCs), in contrast, are available in small portable models and are considered an affordable alternative to the SMPS and APS. An OPC measures the intensity of light scattered from aerosol particles through a focused light that allows illumination of one particle at a time (Hinds 1999). The amount of incident scattered light from a particle is a function of particle size and composition, which can be calibrated using monodisperse particles (Liu et al. 1974). The minimum particle size that can be detected with an OPC depends on the model but generally ranges from 0.1  $\mu\text{m}$  to 0.3  $\mu\text{m}$  (Gao et al. 2016; Szymanski and Liu 1986). Particles smaller than this size scatter little light, making their measurement difficult.

The Portable Aerosol Spectrometer (PAS-1.108; cost \$15,000, GRIMM Aerosol Technixk GmbH & Co., Ainring, Germany) is an OPC designed for both environmental and occupational measurements. The PAS-1.108 (GRIMM 2010) measures particle number concentrations in 15 bins from 0.3  $\mu\text{m}$  to 20  $\mu\text{m}$  and calculates mass concentrations in three particle size fractions (PM<sub>1</sub>, PM<sub>2.5</sub>, and PM<sub>10</sub>). The PAS-1.108 operates with a laser (40 mW max) that alternately scans particles for 3 s at 0.5 mW to detect large particles, and then another 3 s at 30 mW to detect small particles (GRIMM 2010; Grimm and Eatough 2009). The PAS-1.108 has been evaluated in multiple studies for different environments. In a laboratory study, Peters et al. (2006) found the PAS-1.108 to provide similar mass concentration measurements to the APS for polydisperse particles (0.6–20  $\mu\text{m}$ ). For environmental urban settings, Burkart et al. (2010) found the PAS-1.108 total number concentration measurements are correlated ( $\sim R^2 = 0.97$ ) compared to a differential mobility analyzer for particles larger than 0.3  $\mu\text{m}$ . For occupational settings, Cheng (2008) compared the PAS-

1.108 mass concentrations with gravimetric measurements for PM<sub>2.5</sub> and PM<sub>10</sub>, and reported a correlation ( $R^2$ ) of 0.94 and 0.93, respectively.

The OPC-N2 (Alphasense Ltd., cost:  $\sim \$500$ , Essex, United Kingdom) is a low-cost optical particle counter that has recently become available for environmental monitoring. The OPC-N2 (Alphasense 2015) measures particle number concentration in 16 bins from 0.38  $\mu\text{m}$  to 17  $\mu\text{m}$  and calculates mass concentration for three particle sizes (PM<sub>1</sub>, PM<sub>2.5</sub>, and PM<sub>10</sub>). The OPC-N2 contains a laser (25 mW max) that normally operates at a single power between 5 mW and 8 mW (Alphasense 2015). To our knowledge, the OPC-N2 has not been evaluated in any study at the time the article was written.

The objective of this study was to compare the performance of the OPC-N2 to the PAS-1.108 and to reference instruments at different particle sizes, concentrations, and aerosol types. First, we calculated the counting efficiency for both sensors at different particle sizes using monodisperse particles. Then, we evaluated PM<sub>1</sub>, PM<sub>2.5</sub>, and PM<sub>10</sub> from the OPCs to that measured with reference instruments for salt, welding fume, and Arizona road dust (ARD).

## Methods and materials

### OPC instruments

Three OPC-N2 sensors and one PAS-1.108 were used for the current study. The OPC-N2 sensors were new and used for the first time. The PAS-1.108 was sent back to the manufacturer for calibration before conducting the experiment. These OPCs operate on the same physical principles, but are constructed and designed differently as described in Table 1. The PAS-1.108 sizes particles over a wider range (0.3–20  $\mu\text{m}$ ) but fewer bins (15) than the OPC-N2 (0.38–17  $\mu\text{m}$ ; 16 bins). The number counting and sizing of the OPC-N2 was calibrated with monodispersed, polystyrene latex (PSL) particles by the manufacturer. In contrast, the PAS-1.108 is calibrated for different particle sizes with a reference instrument that is calibrated beforehand. The scattering angle and laser wavelengths are different for both devices, however both devices use a mirror to ensure all scattered light is collected by the photodetector. The PAS-1.108 is equipped with a gravimetric filter that allows for determination of a site-specific correction factor (C-factor). This C-factor can be uploaded into the firmware to more accurately adjust instrument response to mass concentration. In contrast, a user of the OPC-N2 must contact the manufacturer to change the default particle density (1650 kg/m<sup>3</sup>) and volume-weighting factor (1.0), which can be set for each size bin. Such correction accounts for

**Table 1.** OPC-N2 and PAS-1.08 specifications.

Technical data	OPC-N2*	PAS-1.108**
Records particle in	Particles per second and milliliter/second	Particles/liter
Number of bins	16	15
Sizing range ( $\mu\text{m}$ )	0.38 to 17	0.3 to 20
Firmware calculated mass concentrations	PM <sub>1</sub> , PM <sub>2.5</sub> , PM <sub>10</sub> ***	PM <sub>1</sub> , PM <sub>2.5</sub> , PM <sub>10</sub>
Particle size calibration method	Direct calibration with monodisperse PSL particles and TSI 3330 OPC (TSI Inc., Shoreview, MN, USA) as the reference instrument	Indirect calibration with a Grimm calibration tower that is calibrated beforehand with monodisperse PSL particles
Mass concentration calibration method	Unknown	Polydisperse dolomite dust and a Grimm calibration tower as the reference instrument
Internal storage capacity	16 GB SD card	4 MB data storage card
Measurement frequency	1 to 10 s	6 s to 1 h
Number concentration range (particles/cm <sup>3</sup> )	1 to 2100	1 to 2000
Mass concentration range ( $\mu\text{g}/\text{m}^3$ )	0.1 to 1500,000	0.1 to 100,000
Particle sensing zone specification		
Scattering angle (degrees)	30	90
Laser maximum power (mW)	25	40
Laser wavelength (nm)	658	780
Light detector	Dual-element photodetector	Photodetector
Mirror to reflect scattered light towards detector	Elliptical mirror	Wide-angle mirror
Internal rechargeable battery	No	Yes
Dimensions [ $L \times W \times H$ ] in meters	0.075 $\times$ 0.0635 $\times$ 0.06	0.24 $\times$ 0.13 $\times$ 0.07
Weight (kg)	0.105	2.4
LCD Screen	No	Yes
Laser lifetime	36 months	4000 h on average

\*Alphasense (2015). \*\*GRIMM (2010). \*\*\*OPC-N2 firmware version at the time the experiments were conducted was OPC-017b.

errors in sizing due to differences in the refractive index of particles used for calibration and those being measured (Jean-Baptiste et al. 2010). Both OPC manufacturers state that the calculation of mass concentration by firmware is proprietary, and thus unknown. Finally, the OPC-N2 is substantially smaller and lighter than the PAS-1.108. Thus, the OPC-N2 can be used as a personal monitor. Much of the extra size and weight of the PAS-1.108 is used for a battery and on-board user interface, which the OPC-N2 does not have.

### Experimental setup

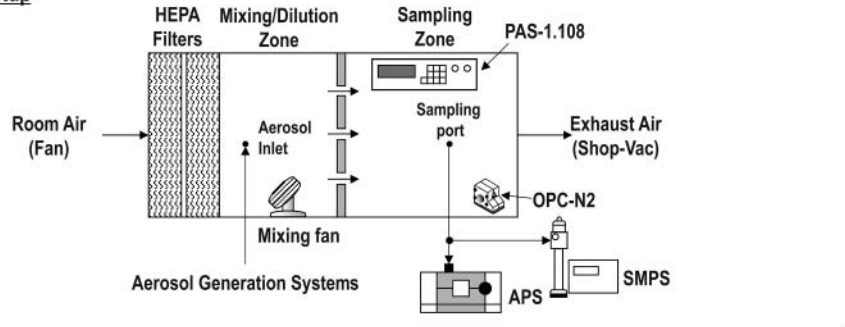
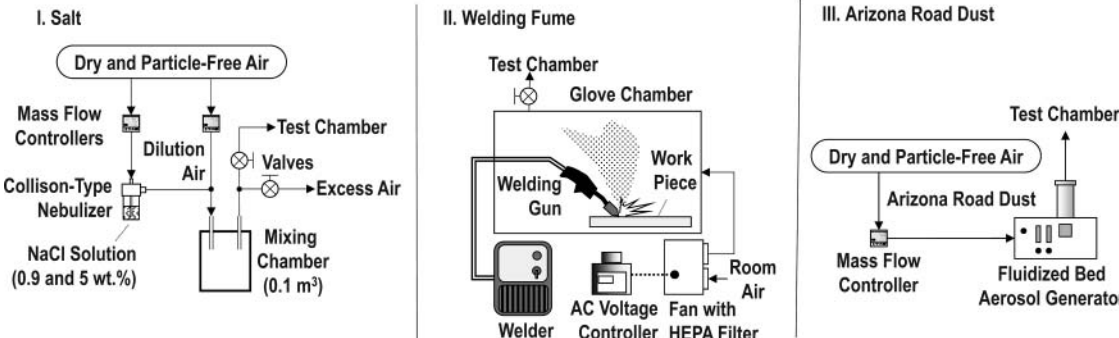
#### Chamber description

The experimental setup is shown in Figure 1a. The test chamber is consisted of a mixing zone (0.64 m  $\times$  0.64 m  $\times$  0.66 m) and a sampling zone (0.53 m  $\times$  0.64 m  $\times$  0.66 m), divided by a perforated plate positioned in the middle of the test chamber. The perforated plate contained 600 evenly spaced holes, each with a diameter of 0.6 cm. The perforated plate allowed for homogenous airflow with no dead zones inside the sampling zone. The aerosol from the generation systems was diluted by clean air from two HEPA filters (0.25 m<sup>3</sup>/min) and mixed with a small fan in the mixing zone. The wind speed in the sampling zone was 0.01 m/s, resulting in a Reynolds number of 400 (laminar flow). The OPC-N2 and PAS-1.108 sensors were positioned in the sampling zone. A 10  $\mu\text{m}$  cyclone was operated at a flow rate of 1.2 liter per minute, and equipped with a 37-mm glass

microfiber filter (934-AH, Whatman, USA) at the outlet. Two reference instruments were outside the test chamber, SMPS C5.402 (GRIMM Aerosol Technik GmbH & Co., Ainring, Germany) and APS 3321 (TSI Inc., Shoreview, MN, USA), directly sampling from the sampling zone. The SMPS was equipped with a 0.804  $\mu\text{m}$  cutoff diameter impactor.

#### Aerosol generation

Three polydisperse aerosols were generated using three different aerosol generation systems as depicted in Figure 1b. Salt is a common test aerosol used to evaluate aerosol instruments and does not absorb light. Welding fume is a critical occupational hazard and is representative of aerosol with high light absorption. ARD is representative of a coarse mineral dust (Curtis et al. 2008) commonly found in environment and occupational settings and used to calibrate direct-reading instruments. Salt aerosols were generated using a Collison-type nebulizer (Carefusion, Middleton, WI, USA) with 0.9% salt solution (mass fractions, Figure 1b(I)). This aerosol was diluted with clean air and mixed in a chamber (0.1 m<sup>3</sup>) to achieve desired concentrations. Welding fumes were generated with a welding system (0.03-inch Flux-Corded MIG Wire, Campbell Hausfeld, USA) operated inside a sandblast cabinet (Item 62454, Central Pneumatic, Byron Center, USA, (Figure 1b(II))). To control concentrations, varying amounts of HEPA filtered air were used to push the fume from the cabinet to the sampling chamber. A fluidized bed aerosol generator (3400A, TSI Inc.,

**A. Experimental Setup****B. Aerosol Generation Systems**

**Figure 1.** Experimental set-up used to determine the performance of the low-cost sensors.

Shoreview, MN, USA) was used to aerosolize Arizona road dust (Fine Grade, Part No. 1543094, Powder Technology INC., Arden Hills, MN) with the concentration adjusted by controlling the feed rate of the dust entering the fluidized bed (Figure 1b(III)).

Aerosol size distribution varied by particle type, but was approximately the same for different concentration levels of the same aerosol type. For each level, the number concentration by size was measured with the SMPS three times after reaching steady-state concentration. A total of six or seven different concentration levels were measured for each aerosol type. The OPC-N2 sensors were set to record every 1-s and the PAS-1.108 was set to record every 6 s. The APS was set to record particles number concentration by size every minute throughout the experiment. The SMPS was set to record every 3 min. Prior to starting experiments, the air in the chamber was confirmed to have low mass concentrations with the OPC-N2 ( $<0.1 \mu\text{g}/\text{m}^3$ ) and the PAS-1.108 ( $<0.1 \mu\text{g}/\text{m}^3$ ).

#### Homogeneity test

Before the experiment, we tested the homogeneity of the sampling zone in Figure 1a, to ensure minimal mass concentration differences throughout the area. Four personal DataRAM's (pDR-1500, Thermo Scientific, TSI Inc., Shoreview, MN, USA) photometers with a  $10 \mu\text{m}$  inlet cyclone (cut-off diameter of  $10 \mu\text{m}$ ) were used with salt and ARD for the current test. The pDR-1500 provides

mass concentrations inferred from flux of light scattered by the assembly of particles that are smaller than the cyclone cut-point. The test was conducted to measure homogeneity in the center and the corners of the sampling zone. Therefore, all photometers were placed in the middle next to each other, then each photometer was placed in a different corner of the sampling zone. For each position (center and corners), measurements were collected for 15 min for each aerosol. To measure precision, the coefficient of variation (CV) was calculated for each minute as follows (NIOSH 2012):

$$CV = \frac{\sigma}{\mu} \quad [1]$$

where  $\sigma$  is the standard deviation and  $\mu$  is the mean of the measurements from the four photometers. The average CV was determined based on the 15 min values calculated for each position. Acceptable CV values for test instruments, according to the EPA, are up to 10% (EPA 2016).

Precision values were acceptable for both positions and both aerosols. For salt, CV values for the center and corner positions were 5.2% and 8.3%, respectively. For ARD, CV values for the center and corner positions were 7.5% and 9.5%, respectively. Although precision was slightly lower for the salt experiment, the CV values for both fine and coarse aerosols were less than 10%. Low precision values provide a good indication that mass

concentrations in the sampling zone of the chamber are homogenous.

### **Detection efficiency**

The detection efficiencies of the OPC-N2 and PAS-1.108 were measured for five sizes (0.5  $\mu\text{m}$ , 0.83  $\mu\text{m}$ , 1.0  $\mu\text{m}$ , 3.0  $\mu\text{m}$ , and 5.0  $\mu\text{m}$ ) of monodispersed PSL particles (Fisher Scientific, Franklin, MA, USA). For each size, a suspension of PSL in distilled water was aerosolized using a vibrating nebulizer (Aerogen, Deerfield, IL, USA), and the aerosol was passed into the sampling zone (Figure 1a). Particle number concentration was measured with the OPCs, APS, and SMPS for 15 min. The SMPS and APS were used to verify the monodispersed particle generation, and to ensure minimal submicrometer aerosol particle sizes from background contamination. The detection efficiency ( $\eta_D$ ) was calculated as follows:

$$\eta_D = \frac{N_{\text{TD}}}{N_{\text{Ref}}} \times 100 \quad [2]$$

where  $N_{\text{TD}}$  is the number concentration measured by the test devices, OPC-N2 or PAS-1.108, and  $N_{\text{Ref}}$  is the number concentration measured by reference instrument. For PSL particles larger than 0.5  $\mu\text{m}$  the APS was used as the reference instrument, and for 0.5  $\mu\text{m}$  PSL particles the SMPS was used as the reference instrument.

### **Response and precision**

The number and mass concentrations output by the OPC-N2 and PAS-1.108 were compared to reference number and mass concentrations for all three aerosols (salt, welding fume, and ARD). Reference mass concentration was measured using both SMPS and APS to cover the entire particle size range. The reference mass concentration summed over all sizes for the SMPS and APS were multiplied by a correction factor calculated with the 37-mm gravimetric filter used with the cyclone. The correction factor was calculated by dividing the mass concentration measured gravimetrically with the mean of unadjusted SMPS and APS mass concentrations over the entire experiment. A new 37-mm filter was used for each aerosol type. Density and shape factor assumptions for SMPS and APS mass calculations were chosen similar to Sousan et al. (2016). The OPC-N2, PAS-1.108, and APS mass concentrations were averaged over 3 min to match the SMPS mass concentrations. The particle number concentration at different particle sizes was compared for the three aerosol types.

For mass concentrations, two different evaluations were performed for OPC-N2 and PAS-1.108. The first was based on the internal firmware real-time mass concentrations recorded from both devices for  $\text{PM}_1$ ,  $\text{PM}_{2.5}$ , and  $\text{PM}_{10}$ . The second was a number to mass concentration calculation of  $\text{PM}_{10}$  based on three assumptions. First, we assumed an unknown aerosol with a density of 1000  $\text{kg}/\text{m}^3$ . Then, we assumed a known aerosol, 2200  $\text{kg}/\text{m}^3$  for salt, 3400  $\text{kg}/\text{m}^3$  for welding fume, and 2650  $\text{kg}/\text{m}^3$  for ARD (Sousan et al. 2016). Welding fume density was assumed as 3400  $\text{kg}/\text{m}^3$  based on Hewett (1995). Finally, we assumed 1650  $\text{kg}/\text{m}^3$  based on the manufacturer recommended density for OPC-N2 (Alphasense 2015). We also assumed that OPCs optical diameter were spheres and equal to the volumetric diameter, therefore no shape factor values were introduced in the mass calculations for both OPCs. We calculated the mass concentration performance for all three particle sizes,  $\text{PM}_1$ ,  $\text{PM}_{2.5}$ , and  $\text{PM}_{10}$ . The comparison for measured and calculated mass included slope, intercept, Pearson coefficient ( $r$ ), coefficient of determination ( $R^2$ ), bias, and precision (CV; for OPC-N2 only). The evaluation was performed in the same manner done by Sousan et al. (2016), following the acceptance criteria for EPA and NIOSH.

## **Results**

### **Detection efficiency**

The detection efficiency by size of the OPC-N2 and PAS-1.108 for monodispersed PSL particles is shown in Figure 2. For particles larger than 0.8  $\mu\text{m}$ , the detection efficiency of the OPC-N2 (range 83–101%) was slightly higher and nearer to 100% than the PAS-1.108 (range 79–90%). The detection efficiency of both OPCs was near 100% for 0.8- $\mu\text{m}$  particles, decreased for 1.0- $\mu\text{m}$  particles, and then increased again for 3.0- $\mu\text{m}$  and 5.0- $\mu\text{m}$  particles. In contrast for 0.5- $\mu\text{m}$  particles, the detection efficiency of the OPC-N2 (78%) was substantially lower than that of the PAS-1.108 (183%). The efficiency decrease at 1.0- $\mu\text{m}$  was not expected and it is not clear why this happened.

The manufacturer-reported and measured sizes of the PSL particles are listed in Table S1 in the online supplemental information (SI). The bin range diameters of the OPCs that contained the highest number concentration are reported. The corresponding mode diameter, median diameter, and geometric standard deviation were reported for the reference instruments. The median diameters of the reference instruments were within the bin range diameters for the OPC-N2 and PAS-1.108. The bin range diameters from both OPCs were the same

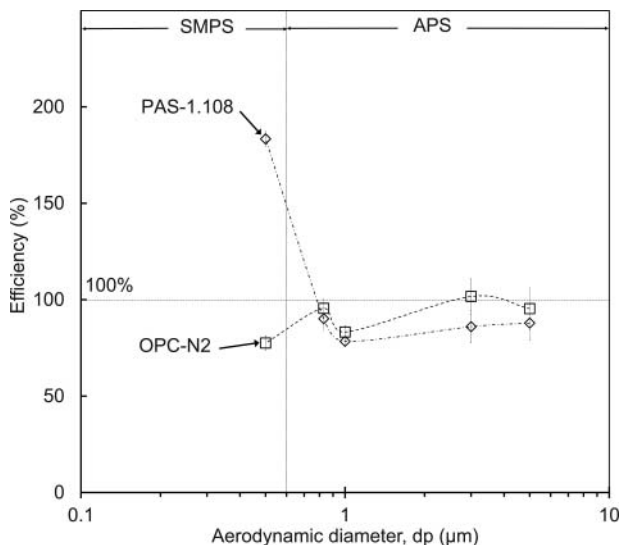


**Figure 2.** Detection efficiency of the OPC-N2 and PAS-1.108 by aerodynamic diameter.

for all PSL sizes, except for 0.5- $\mu\text{m}$  PSL. For this size, the bin range diameters from the OPC-N2 (0.38–0.54  $\mu\text{m}$ ) were smaller than that from the PAS-1.108 (0.5–0.65  $\mu\text{m}$ ). Both OPCs detected the highest number concentration with a mid-point diameter of 0.9  $\mu\text{m}$  for the 0.83- $\mu\text{m}$  and 1.0- $\mu\text{m}$  PSL.

### Response and precision

#### Number concentrations

Normalized particle number concentration by size measured with the OPCs and reference instruments for the three aerosols are shown in Figure 3. The *y*-axis is normalized by dividing the number concentration for each bin by the width of the bin (logged) and accounts for the fact that the bin widths are not equal in size for the SMPS and APS. The result is called a lognormal distribution that helps correct the distorted skewness exhibited over the large particle range caused by the normal distribution (Hinds 1999). These size distributions are plotted by volumetric particle diameter to allow direct comparison among instruments and shown with a log-log scale to allow high number concentrations measured with the SMPS to be visible with the other instruments. The *x*-axis on each graph starts from 0.1  $\mu\text{m}$  to visually concentrate on the area of interest for instrument comparison. We plotted the size distribution for the highest concentrations (total mass concentrations according to the reference devices were 1960  $\mu\text{g}/\text{m}^3$  for salt, 9860  $\mu\text{g}/\text{m}^3$  for welding fume, and 3550  $\mu\text{g}/\text{m}^3$  for ARD). The size distributions were an average of 9-min measurements from the OPCs and the reference instruments and were representative of lower concentrations. For each aerosol, number and mass

fraction by size from SMPS and APS data for experiments conducted at low and high concentrations were similar (Figure S1 for number fraction and Figure S2 for mass fraction, in the SI). The only difference observed is for welding fume mass concentration, where the size distribution becomes multi-modal for high concentrations (Figure S2b).

In general, the two OPCs measured similar number concentrations that decreased with increasing particle size consistent with SMPS and APS measurements, although there were substantial differences dependent on aerosol type. For salt (Figure 3a), the number concentrations measured with the OPC-N2 were lower than those measured with the APS for particles smaller than 1  $\mu\text{m}$ , but similar for larger particles. In contrast, both OPCs were substantially higher than the number concentrations measured with the SMPS for particles smaller than 1  $\mu\text{m}$ . The number concentrations measured with PAS-1.108 were lower than those measured with the APS for particle sizes between 0.7  $\mu\text{m}$  and 1.5  $\mu\text{m}$  but similar for particles larger than 1.5  $\mu\text{m}$ . For particles smaller than 0.7  $\mu\text{m}$ , the PAS-1.108 number concentrations were higher than those from the SMPS or APS.

For welding fume (Figure 3b), the results for the OPC-N2 were similar to those reported for salt above. However, the number concentrations measured with the PAS-1.108 were lower than those measured with the APS for all particle sizes 0.57  $\mu\text{m}$  and larger. Also, the PAS-1.108 number concentrations were higher than the SMPS for particles smaller than 0.5  $\mu\text{m}$ . The SMPS measurements for welding fume have a smaller range (up to 0.26  $\mu\text{m}$ ) than salt (Figure 3b) because the high shape factor value (welding fume = 3.9) causes the mid-point mobility diameter for the largest size channel of the SMPS to be converted from 1.0  $\mu\text{m}$  to 0.26  $\mu\text{m}$  (volumetric diameter). Substantially, different results were obtained for the coarse ARD (Figure 3c). The number concentrations measured by the OPC-N2 were higher than those measured with the SMPS and APS, except for 0.65- $\mu\text{m}$  particles. The number concentrations measured with the PAS-1.108 were also higher than those measured with the SMPS and APS, except for 1.3- $\mu\text{m}$  and 0.73- $\mu\text{m}$  particles. It is noteworthy to mention that OPC-N2 and PAS-1.108 both gave identical number concentrations as the SMPS and APS for particle sizes of 0.73  $\mu\text{m}$ , 0.9  $\mu\text{m}$ , and 4.5  $\mu\text{m}$ .

#### Mass concentrations from firmware

The evaluation of mass concentrations from the OPC firmware ( $\text{PM}_1$ ,  $\text{PM}_{2.5}$ , and  $\text{PM}_{10}$ ) compared to those from reference instruments (gravimetrically-corrected SMPS+APS) is summarized in Table 2. For linear regression, a slope of 1, intercept of 0, *r* of 1, and *R*<sup>2</sup> of 1

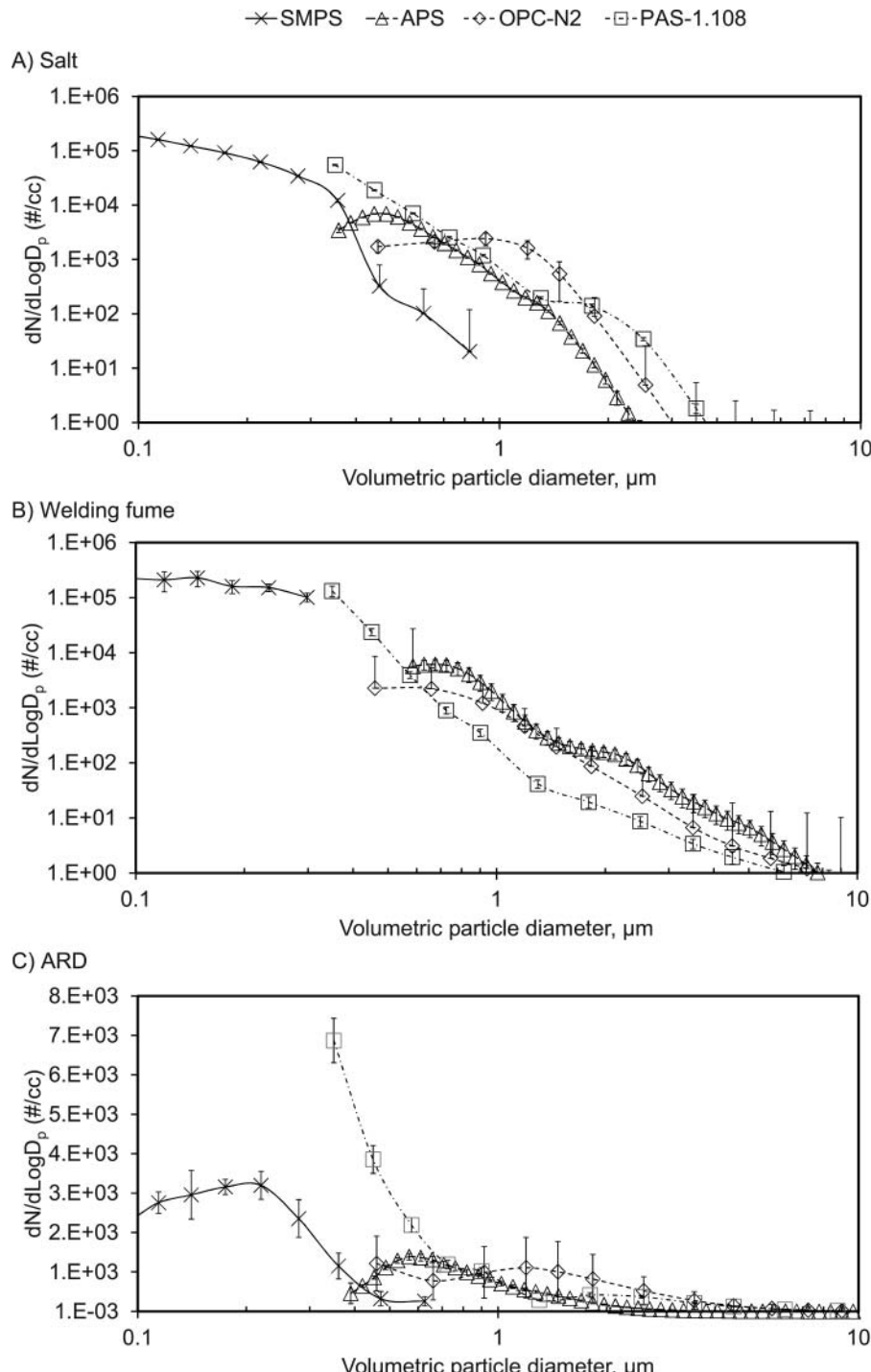


**Figure 3.** Particle number concentration by size measured for (a) salt; (b) welding fume; (c) ARD.

indicate a perfect linear relationship. EPA and NIOSH standards are a slope of  $1 \pm 0.1$ , a  $y$ -intercept of  $0 \pm 5 \mu\text{g}/\text{m}^3$  (EPA only), and an  $r \geq 0.97$  (EPA 2006; NIOSH 2012). Percentage bias is a parameter used by NIOSH to indicate how well a direct-reading instrument agrees with a reference device with  $\pm 10\%$  considered acceptable. Lastly, %CV is an indicator of precision among duplicate instruments, where values less than 10% are

considered acceptable (EPA 2016). CV values were not calculated for PAS-1.108 because only one instrument was available. Selected information is depicted in scatter-plots of firmware-calculated mass concentrations relative to those from reference instruments (SMPS + APS) in Figure 4 for salt aerosol ( $\text{PM}_{1}$ ,  $\text{PM}_{2.5}$ , and  $\text{PM}_{10}$ ) and in Figure 5 for welding fume and ARD ( $\text{PM}_{10}$  only). In these figures, the  $x$ -axis error bars (the standard

**Table 2.** Evaluation of firmware-calculated mass concentrations from the OPC-N2 and PAS-1.108 with reference to gravimetrically-corrected SMPS and APS data for (a) PM<sub>1</sub>, (b) PM<sub>2.5</sub>, and (c) PM<sub>10</sub>.

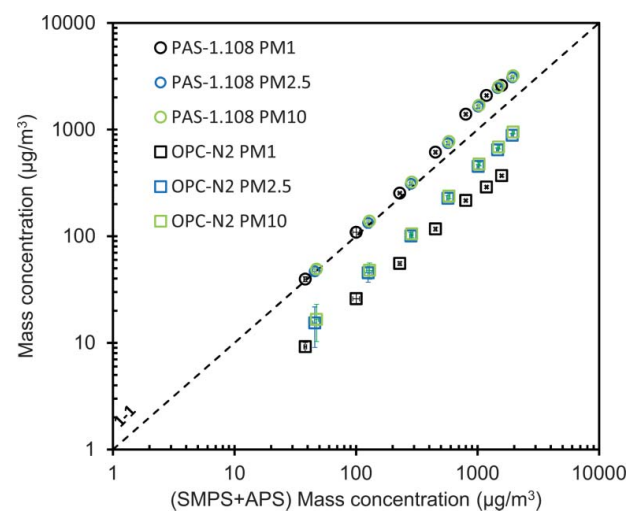
Instrument	Data Pairs	Slope $\pm$ Std. Error	Intercept $\pm$ Std. Error ( $\mu\text{g}/\text{m}^3$ )	<i>r</i>	<i>R</i> <sup>2</sup>	% Bias	% CV
(a) PM <sub>1</sub>							
Salt							
OPC-N2	8	0.2 $\pm$ 0.006	3.9 $\pm$ 5.0 <sup>1</sup>	0.99 <sup>1,2</sup>	0.99	-70	6.6 <sup>1</sup>
PAS-1.108	8	1.7 $\pm$ 0.06	-58 $\pm$ 43	0.99 <sup>1,2</sup>	0.99	30	—
Welding fume							
OPC-N2	7	0.03 $\pm$ 0.003	0.7 $\pm$ 9.6 <sup>1</sup>	0.97 <sup>1,2</sup>	0.94	-92	9.5 <sup>1</sup>
PAS-1.108	7	0.6 $\pm$ 0.05	-255 $\pm$ 159	0.98 <sup>1,2</sup>	0.97	-61	—
ARD							
OPC-N2	7	0.6 $\pm$ 0.02	5.0 $\pm$ 2.6 <sup>1</sup>	0.99 <sup>1,2</sup>	0.99	-19	15
PAS-1.108	7	1.7 $\pm$ 0.03	6.0 $\pm$ 4.0	0.99 <sup>1,2</sup>	0.99	72	—
(b) PM <sub>2.5</sub>							
Salt							
OPC-N2	8	0.5 $\pm$ 0.008	-15 $\pm$ 7	0.99 <sup>1,2</sup>	0.99	-57	4.8
PAS-1.108	8	1.7 $\pm$ 0.04	-75 $\pm$ 43	0.99 <sup>1,2</sup>	0.99	25	—
Welding fume							
OPC-N2	7	0.04 $\pm$ 0.005	-19 $\pm$ 18	0.97 <sup>1,2</sup>	0.94	-91	8.7
PAS-1.108	7	0.5 $\pm$ 0.03	-226 $\pm$ 131	0.99 <sup>1,2</sup>	0.98	-65	—
ARD							
OPC-N2	7	0.9 $\pm$ 0.02	24 $\pm$ 16	0.99 <sup>1,2</sup>	0.99	-1.9	14
PAS-1.108	7	1.1 $\pm$ 0.02	15 $\pm$ 12	0.99 <sup>1,2</sup>	0.99	6.9	—
(c) PM <sub>10</sub>							
Salt							
OPC-N2	8	0.5 $\pm$ 0.009	-18 $\pm$ 9.0	0.99 <sup>1,2</sup>	0.99	-55	4.2
PAS-1.108	8	1.7 $\pm$ 0.04	-79 $\pm$ 43	0.99 <sup>1,2</sup>	0.99	27	—
Welding fume							
OPC-N2	7	0.05 $\pm$ 0.005	-17 $\pm$ 23	0.98 <sup>1,2</sup>	0.96	-89	6.1
PAS-1.108	7	0.4 $\pm$ 0.03	-215 $\pm$ 134	0.99 <sup>1,2</sup>	0.98	-67	—
ARD							
OPC-N2	7	1.6 $\pm$ 0.04	105 $\pm$ 72	0.99 <sup>1,2</sup>	0.99	63	16
PAS-1.108	7	2.7 $\pm$ 0.04	85 $\pm$ 73	0.99 <sup>1,2</sup>	0.99	147	—

<sup>1</sup>Meets EPA criterion.<sup>2</sup>Meets NIOSH criterion.

deviation of SMPS and APS measurements) indicate the variability of mass concentration at each steady state, whereas the *y*-axis error bars (the standard deviation within OPC-N2 and PAS-1.108) indicate a combination of within-sensor precision (OPC-N2 only) and concentration variability. Both figures are on a log-log scale to visually capture both low and high-mass concentrations.

For all aerosols and PM metrics, the firmware-calculated PM<sub>1</sub>, PM<sub>2.5</sub>, and PM<sub>10</sub> from both OPCs were highly linear with those measured by the reference devices. All *r*-values were greater than 0.97, meeting EPA and NIOSH criteria. However, substantial variation was observed in slope by aerosol and PM metric, ranging from 0.03 (welding fume, OPC-N2, PM<sub>1</sub>) to 2.7 (ARD, PAS-1.108, PM<sub>10</sub>). For the OPC-N2, slopes for PM<sub>1</sub> and PM<sub>10</sub> did not meet performance criteria (EPA and NIOSH criteria) for all three aerosols and ranged from 0.03 to 1.6. For PM<sub>2.5</sub>, the slope value was 0.9 for ARD, but did not meet performance criteria for salt and welding fume. Intercept values for PM<sub>2.5</sub> and PM<sub>10</sub> did not meet EPA performance criteria for all aerosols, ranging from -19  $\mu\text{g}/\text{m}^3$  to 105  $\mu\text{g}/\text{m}^3$ . For PM<sub>1</sub>, intercept values were within 0  $\pm$  5  $\mu\text{g}/\text{m}^3$  for all aerosols and

approached zero. Bias values for PM<sub>1</sub> and PM<sub>10</sub> did not meet performance criteria (EPA and NIOSH criteria) for all aerosols and ranged from -92% to 63%. Bias value for PM<sub>2.5</sub> was low for ARD at -1.9%, but did not meet

**Figure 4.** Firmware calculated PM<sub>1</sub>, PM<sub>2.5</sub>, and PM<sub>10</sub> mass concentrations for OPC-N2 and PAS-1.108 relative to reference mass concentration for the salt experiment.

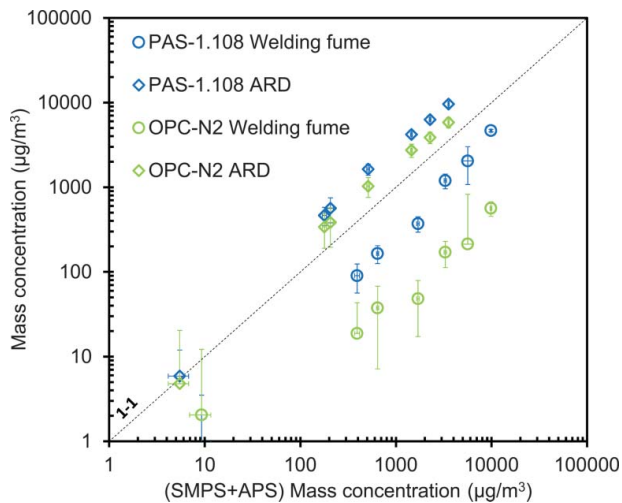


**Figure 5.** Firmware calculated PM<sub>10</sub> mass concentrations for OPC-N2 and PAS-1.108 relative to reference mass concentration for welding fume (circles) and ARD (diamonds) experiments.

performance criteria for salt and welding fume and ranged from  $-91\%$  to  $-57\%$ .

For the PAS-1.108, slopes for PM<sub>1</sub> and PM<sub>10</sub> did not meet performance criteria for all three aerosols and ranged from 0.4 to 2.7. For PM<sub>2.5</sub>, the slope was 1.1 for ARD, but did not meet performance criteria for salt and welding fume. Intercepts for PM<sub>1</sub>, PM<sub>2.5</sub>, and PM<sub>10</sub> did not meet performance criteria for all aerosols and ranged from  $-255\text{ }\mu\text{g/m}^3$  to  $85\text{ }\mu\text{g/m}^3$ . Bias values for PM<sub>1</sub> and PM<sub>10</sub> did not meet performance criteria for all aerosols and ranged from  $-67\%$  to  $147\%$ . Bias value for PM<sub>2.5</sub> was low for ARD at 6.9%, but did not meet performance criteria for salt and welding fume and ranged from  $-65\%$  to 25%.

The precision was high for OPC-N2 with CVs for PM<sub>1</sub>, PM<sub>2.5</sub>, and PM<sub>10</sub> lower than 10% (EPA criteria) for salt and welding fume (range from 4.2% to 9.5%). The precision (CV) values for PM<sub>1</sub>, PM<sub>2.5</sub>, and PM<sub>10</sub> were higher than 10% for ARD (range from 14% to 16%). For ARD, the precision values were higher than EPA standards, but CV values were only 6% higher than recommended.

#### Mass concentrations calculated from number concentrations

The evaluation of PM<sub>10</sub> calculated from number concentration by size measured with the OPC-N2 and PAS-1.108 are summarized in Table 3. Regardless of assumptions made in calculations or aerosol type, the relationships among PM<sub>10</sub> calculated with number concentration data from the OPCs were linear with that measured with reference instruments ( $r = 0.99$ ). The slopes for OPC-N2 and PAS-1.108 did not meet

performance criteria for all three aerosols and ranged from 0.05 to 3.9. The slope values for both OPCs were similar for all three assumptions and different aerosols. For example, for a known type aerosol (Table 3b), the OPC-N2 slope values were 0.7, 0.2, and 3.9, and the PAS-1.108 slope values were 0.8, 0.3, and 3.6, for salt, welding fume, and ARD, respectively. Slope values also show that mass concentrations measured by both OPCs were low for salt and welding fume, and high for ARD. Intercept values for OPC-N2 and PAS-1.108 did not meet performance criteria and were different for all three aerosols, ranging from  $-111$  to  $432\text{ }\mu\text{g/m}^3$ . Compared to mass concentrations measured with reference instruments, bias values did not meet performance criteria for both instruments and all aerosols and ranged from  $-92$  to  $168\%$ . PM<sub>10</sub> calculations were chosen as a representative example for PM<sub>1</sub> and PM<sub>2.5</sub>. Finally, the calculated mass concentrations based on the three assumptions in Table 3 did not improve the results to meet EPA and NIOSH standards.

#### Discussion

The OPC-N2 generally provides similar information to the PAS-1.108, and differences in their response may be attributed to detection efficiency. The OPCs sized particles identically and in good agreement with the reference instruments (Table S1). For particles larger than  $0.8\text{ }\mu\text{m}$ , the finding that number concentrations measured with the OPC-N2 were similar to or higher than those measured with the PAS-1.108 (Figure 3) is consistent with the OPC-N2 having slightly higher detection efficiencies for this size range (Figure 2). Conversely, for smaller particles, number concentrations were underestimated with the OPC-N2 compared to the PAS-1.108 and reference instruments. This finding is also consistent with the OPC-N2 having a substantially lower detection efficiency compared with the PAS-1.108 that overestimates number concentration for  $0.5\text{-}\mu\text{m}$  particles.

Differences in detection efficiency may relate to the way the lasers are operated within the devices or calibration procedures. As stated in the manual (Alphasense 2015), the laser (25 mW maximum power) in the OPC-N2 normally operates between 5 mW and 8 mW. In contrast, the laser (40 mW maximum power) in the PAS-1.108 operates at 0.5 mW for 3 s to optimize sensing of particles larger than  $2\text{ }\mu\text{m}$  and then at 30 mW for another 3 s to enhance the intensity of scattering light by particles smaller than  $2\text{ }\mu\text{m}$  (GRIMM 2010). The firmware then combines these data into a single particle size distribution that is measured every 6 s. The modulation to a higher power to detect smaller particles may explain why the PAS-1.108 has a substantially higher detection

**Table 3.** Evaluation of  $PM_{10}$  calculated from number concentration by size measured by the OPC-N2 and PAS-1.108 based on: (a) unknown aerosol type with density = 1000 kg/cm<sup>3</sup>; (b) known aerosol type; (c) OPC-N2 manufacturer recommended density of 1650 kg/cm<sup>3</sup>. Reference concentrations were calculated based on the known aerosol type.

Instrument	Data Pairs	Slope $\pm$ Std. Error	Intercept $\pm$ Std. Error ( $\mu\text{g}/\text{m}^3$ )	<i>r</i>	<i>R</i> <sup>2</sup>	% Bias
(a) Unknown aerosol type (density = 1000 kg/cm <sup>3</sup> )						
Salt						
OPC-N2	8	0.3 $\pm$ 0.006	-12 $\pm$ 5.9	0.99 <sup>1,2</sup>	0.99	-69
PAS-1.108	8	0.4 $\pm$ 0.008	-17 $\pm$ 7.6	0.99 <sup>1,2</sup>	0.99	-63
Welding fume						
OPC-N2	7	0.05 $\pm$ 0.002	-5.6 $\pm$ 12	0.99 <sup>1,2</sup>	0.99	-89
PAS-1.108	7	0.08 $\pm$ 0.004	-33 $\pm$ 20	0.99 <sup>1,2</sup>	0.99	-88
ARD						
OPC-N2	7	1.5 $\pm$ 0.07	163 $\pm$ 112	0.99	0.99	61
PAS-1.108	7	1.4 $\pm$ 0.03	73 $\pm$ 53	0.99	0.99	32
(b) Known aerosol type						
Salt (density = 2200 kg/cm <sup>3</sup> )						
OPC-N2	8	0.7 $\pm$ 0.01	-26 $\pm$ 12	0.99 <sup>1,2</sup>	0.99	-41
PAS-1.108	8	0.8 $\pm$ 0.02	-38 $\pm$ 17	0.99 <sup>1,2</sup>	0.99	-29
Welding fume (density = 3400 kg/cm <sup>3</sup> )						
OPC-N2	7	0.2 $\pm$ 0.008	-19 $\pm$ 39	0.99 <sup>1,2</sup>	0.99	-80
PAS-1.108	7	0.3 $\pm$ 0.01	-111 $\pm$ 69	0.99 <sup>1,2</sup>	0.99	-75
ARD (density = 2650 kg/cm <sup>3</sup> )						
OPC-N2	7	3.9 $\pm$ 0.2	432 $\pm$ 299	0.99	0.99	323
PAS-1.108	7	3.6 $\pm$ 0.08	193 $\pm$ 141	0.99	0.99	248
(c) Based on OPC-N2 manufacturer recommended density (density = 1650 kg/cm <sup>3</sup> )						
Salt						
OPC-N2	8	0.5 $\pm$ 0.01	-20 $\pm$ 9.7	0.99 <sup>1,2</sup>	0.99	-54
PAS-1.108	8	0.6 $\pm$ 0.01	-29 $\pm$ 12	0.99 <sup>1,2</sup>	0.99	-45
Welding fume						
OPC-N2	7	0.08 $\pm$ 0.005	-13 $\pm$ 26	0.99 <sup>1,2</sup>	0.98	-92
PAS-1.108	7	0.1 $\pm$ 0.009	-62 $\pm$ 44	0.99 <sup>1,2</sup>	0.98	-89
ARD						
OPC-N2	7	2.5 $\pm$ 0.1	269 $\pm$ 18	0.99	0.99	168
PAS-1.108	7	2.2 $\pm$ 0.05	120 $\pm$ 88	0.99	0.99	122

<sup>1</sup>Meets EPA criterion.

<sup>2</sup>Meets NOISH criterion.

efficiency than the OPC-N2 for 0.5- $\mu\text{m}$  PSL (Figure 2). Conversely, the fact that the OPC-N2 operates at a higher minimum power (5 mW) than the PAS-1.108 (0.5 mW) may explain why detection efficiency is higher for particles larger than 2  $\mu\text{m}$ . However, different calibration procedures may also partially explain the different detection efficiencies.

Number concentration measurements by both OPCs for all three aerosol types agreed well with the detection efficiency results. For particles larger than 0.8  $\mu\text{m}$ , the OPC-N2 measured similar or higher number concentrations compared to the PAS-1.108 for all three aerosols, as shown in Figure 3. Compared to the reference instrument, both OPCs underestimated number concentration measurements for salt and welding fume and overestimated number concentration measurements for ARD. For coarse particles, both OPCs agreed well, especially for ARD. For particles smaller than 0.8  $\mu\text{m}$ , the number concentration measurements from both OPCs were different. The OPC-N2 underestimated number concentration and the PAS-1.108 overestimated number concentration compared to the reference instrument. In some cases, the number concentration of the SMPS and

APS did not match well in the size range, where the instruments overlap (0.5–0.8  $\mu\text{m}$ ). One reason is that the instruments use different principles; the SMPS uses the electrical mobility (Wang and Flagan 1990) and the APS uses time-of-flight between two narrow laser beams (Armendariz and Leith 2002).

These results are consistent with other researcher's results. For ARD, Peters et al. (2006) found that number concentrations measured with the PAS-1.108 were higher than those from the APS for particles smaller than 0.7  $\mu\text{m}$  and larger than 2.0 (aerodynamic diameter). Measuring urban air, Burkart et al. (2010) reported that number concentrations measured with the PAS-1.108 were 9% higher than the DMA for particles larger than 0.3  $\mu\text{m}$ . Belosi et al. (2013) found that number concentrations measured with the PAS-1.108 were higher than those from a Las-X active cavity laser for all particle sizes, except for the 0.6- $\mu\text{m}$  particle size. In contrast, for large particles, we observed PAS-1.108 underestimation for salt and welding fume since both aerosols consist small particles.

For all aerosols, the mass concentrations from the firmware of the OPC-N2 and PAS-1.108 were highly

linear with that measured by reference instruments ( $r > 0.97$ ), although the slopes varied dramatically by OPC type and PM size fraction (Table 2; Figures 4 and 5). For salt (Figure 4), mass concentrations estimated from OPC-N2 firmware were substantially lower than the mass concentrations measured with the reference instruments with the magnitude of departure dependent on PM metric ( $PM_1$  slope = 0.2;  $PM_{2.5}$  slope = 0.5;  $PM_{10}$  slope = 0.5). In contrast, the situation was opposite for the PAS-1.108 with mass concentrations over-estimated by the same magnitude for all metrics ( $PM_1$  slope = 1.7;  $PM_{2.5}$  slope = 1.7;  $PM_{10}$  slope = 1.7). The salt aerosol was dominated by submicrometer aerosols (Figure 3a) in a size range over which the OPC-N2 has a detection efficiency less than 100% (Figure 2, 78% at 0.5  $\mu\text{m}$ ) and the PAS-1.108 greater than 100% (183% at 0.5  $\mu\text{m}$ ). Consequently, the finding of slopes less than 1 for the OPC-N2 and greater than 1 for the PAS-1.108 can be attributed to differences in OPC detection efficiencies for small particles. Moreover, this issue becomes more apparent for the  $PM_1$  metric because of the inability of the OPC-N2 to adequately detect sub-0.8-micrometer particles. The fact that the OPC-N2 and PAS-1.108 respond differently for different aerosol types relates to differences in particle size and optical properties (Sousan et al. 2016).

A similar but more extreme situation was apparent for the welding fume. The slopes for the OPC-N2 (Table 2;  $PM_1$  slope = 0.03 and  $PM_{10}$  slope = 0.05) were consistently and substantially lower than that of the PAS-1.108 (range: 0.6 for  $PM_1$  to 0.4 for  $PM_{10}$ ). These differences can again be attributed to the fact that the OPC-N2 has a dramatically lower detection efficiency than the PAS-1.108 for submicrometer aerosols. The finding that for a given OPC and PM metric, the slopes for welding fume were much lower than for salt (e.g., for the PAS-1.108,  $PM_{10}$  slope was 0.4 for welding fume and 1.7 for salt) may be due to differences in particle detection efficiency or refractive index by aerosol type. However, the fraction of particles smaller than the typical detection limit of OPCs was slightly more for salt aerosol (91% by number and 18% by mass less than 0.2  $\mu\text{m}$ ; Figure S1) than for welding fume (86% by number and 13% by mass less than 0.2  $\mu\text{m}$ ; Figure S2). Consequently, we cannot attribute the differences in slopes with aerosol type to the lack of small particles being detected. Instead, we believe that these differences were caused by the fact that the refractive index for welding fume has an absorbing component. The absorbing component of welding fume particles is known to cause particles to be undersized (Syvitski 2007). Even small errors in undersizing of particles can lead to large errors in estimates of mass concentration because the mass concentration is proportional to the particle diameter cubed.

In contrast to salt and welding fume, the slopes for ARD were highly variable for the OPC-N2 (Table 2;  $PM_1$  slope = 0.6;  $PM_{2.5}$  slope = 0.9;  $PM_{10}$  slope = 1.6) and PAS-1.108 ( $PM_1$  slope = 1.7;  $PM_{2.5}$  slope = 1.1;  $PM_{10}$  slope = 2.7). For the ARD, larger particles were a much more important contributor to the aerosol than salt or welding fume (Figure 3). Thus, a focus on the  $PM_{10}$  metric may be most instructive, which is depicted for ARD and welding fume in Figure 5. The finding that the slopes for firmware-calculated  $PM_{10}$  were both substantially greater than unity is consistent with the overcounting of large particles that can be seen in Figure 3c. The reason for this discrepancy is unknown, although this observation is consistent with that of Peters et al. (2006). They conjectured that large ARD particles may be broken into smaller particles due to the impaction on the walls of the APS acceleration nozzle, thereby shifting the number distribution measured by the APS to smaller sizes.

Other researchers have observed that mass concentrations from OPCs are highly linear with measurements made with filter-based or equivalent methods. In an iron foundry, Cheng (2008) found that firmware-estimated mass concentrations from a PAS-1.108 were highly correlated to those made with a gravimetric sampler (Dichotomous Sampler 241; Thermo Scientific) with a coefficient of determination ( $R^2$ ) of 0.94 for  $PM_{2.5}$  and 0.93 for  $PM_{10}$  for mass concentrations up to 400  $\mu\text{g}/\text{m}^3$ . Parker et al. (2008) reported the mass concentrations from a PAS-1.108 compared to those measured with a tapered element oscillating microbalance had an  $R^2$  of 0.76 when sampling was conducted inside and 0.5 when sampling was conducted in an urban environment (concentrations up to 60  $\mu\text{g}/\text{m}^3$ ). Giorio et al. (2013) reported  $R^2$  values of 0.8, 0.97, and 0.98 for  $PM_1$ ,  $PM_{2.5}$ , and  $PM_{10}$ , respectively, in an urban environment. The fact that we observed similar or higher  $R^2$  values in our study (Table 2, 0.94–0.99) is likely attributed to the fact that our study was conducted in a controlled chamber environment with a single aerosol source opposed to an uncontrolled environment with multiple sources.

Other researchers have also found that the relationship between PM measured with OPCs and filter-based or equivalent samplers are highly impacted by aerosol type and size distribution. In a cast factory, Cheng (2008) found that the slope between the PAS-1.108 and gravimetric measurements were 0.67 and 0.72 for  $PM_{2.5}$  and  $PM_{10}$ , respectively. In an urban environment, Giorio et al. (2013) found that the slope between PM measured with the PAS-1.108 and with a gravimetric sampler was dependent on PM metric (1.4, 1.3, and 1.2 for  $PM_1$ ,  $PM_{2.5}$ , and  $PM_{10}$ , respectively). The mass concentrations measured by both OPCs were higher than those from reference instruments for ARD but lower than reference



instruments for welding fume. Peters et al. (2006) also observed that mass concentrations from the PAS-1.108 were overestimated compared to the APS for ARD.

Inconsistencies between calculated mass concentration from number concentration (Table 3) and mass estimates made with internal firmware (Table 2) are noticeable for both OPCs. Regardless of the density assumptions, the calculated mass concentrations did not match the firmware mass concentrations. For example, for ARD, OPC-N2, and PAS-1.108 slope values in Table 2c change from 1.6 and 2.7 to 3.9 and 3.6, respectively, in Table 3b. Intercept values for OPC-N2 and PAS-1.108 in Table 2c change from 105 and 85  $\mu\text{g}/\text{m}^3$  to 432 and 193  $\mu\text{g}/\text{m}^3$ , respectively. Finally, bias values for OPC-N2 and PAS-1.108 in Table 2c change from 63% and 147% to 323% and 248%, respectively. Similar changes are noticed between Table 2c and Table 3b for salt and welding fume. The differences between both Tables 2 and 3 could be because that the PAS-1.108 firmware calculation uses calibration curves derived with polydisperse dolomite dust (GRIMM 2010). Also, the PAS-1.108 mass calculation is based on 16 channels, where it uses an additional 0.23  $\mu\text{m}$  channel to extrapolate mass concentration by adjusting values through a lognormal distribution (GRIMM 2010). This could explain why PAS-1.108 has higher mass concentrations for all aerosols (Figures 4 and 5) and can calculate mass concentrations for smaller particles, observed for welding fume in Figure 5. Although not mentioned in the manual, and from differences mentioned between Tables 2 and 3, the OPC-N2 clearly utilizes a proprietary calibration curve internally in its firmware mass concentration calculations.

This work emphasizes the need for aerosol-specific correction factors developed with side-by-side measurements made with gravimetric samplers to improve PM estimates made with either the OPC-N2 or PAS-1.108. The PAS-1.018 (GRIMM 2010) is equipped with a 47-mm gravimetric filter in the outlet of the sensor to collect aerosol particles. The PAS-1.108 manual advises the use of the gravimetric filter at any new measurement site to calculate a correction factor (C-factor) that can be used by the sensors firmware to correct mass concentrations. In contrast, the OPC-N2 allows you change the density and volume weighting factors for each size bin that is applied in the mass calculation for each bin (Alphasense 2015). The user can change these weighting factors after contacting the company. The differences between all PM sizes can be seen in Table 2a and Figure 4, where  $\text{PM}_1$  slope value is 0.2 compared to the 0.5 for  $\text{PM}_{2.5}$  and  $\text{PM}_{10}$ . The default weighting factors for each bin is 1.0 and the density is constant, thus the reason for the slope differences must be the proprietary calibration curves used for mass concentration calculation.

The limitation in this study was our density and shape factor assumptions for welding fume that introduced uncertainties in reference mass concentrations from SMPS and APS data. Particles larger than 300 nm were assumed to have a constant shape factor, although Kim et al. (2009) reported that shape factor increases with particle size for welding fume. In addition, welding fume agglomerates can have substantially lower densities (Cena et al. 2014). However, the use of gravimetric filter correction limits the problem. The accuracy and bias results are based on high concentrations that are not typical of ambient mass concentrations in many locations. Future work is needed to evaluate the OPC-N2 at lower mass concentrations. In addition, our chamber experiments were conducted in a controlled environment over a narrow range of temperature and relative humidity, which is typical for many occupational settings. However, future work is needed to elucidate the effect of temperature and relative humidity on the mass concentration measured with the OPC-N2. Finally, our evaluation was performed with new sensors. More work is needed to assess OPC-N2 performance over time (i.e., days, weeks, months).

## Conclusion

We evaluated the ability of the OPC-N2 and PAS-1.108 to measure particle number concentrations by size and mass concentrations ( $\text{PM}_1$ ,  $\text{PM}_{2.5}$ , and  $\text{PM}_{10}$ ) for salt, welding fume, and ARD. The detection efficiencies of both OPCs were similar for particles larger than 0.8  $\mu\text{m}$  (83–101% for the OPC-N2 and 79 to 90% for the PAS-1.108), but diverged substantially for 0.5- $\mu\text{m}$  particles (78% for the OPC-N2 and 183% for the PAS-1.108). Consistent with these detection efficiency observations, the number concentrations measured with the OPC-N2 agreed fairly well to those measured with the PAS-1.108 and reference instruments for coarse particles but underestimated number concentrations for sub-micrometer particles. Mass concentrations from both OPCs firmware were highly linear with the reference instruments ( $>0.97$ ). The precision values for OPC-N2 ranged from 4.2% for salt to 16% for ARD. Calculated mass concentrations from number concentrations did not agree with the firmware mass concentrations, which could be due to the proprietary internal calibration curves used to correct mass calculations. The OPC-N2 and PAS-1.108 would be a good choice for measuring aerosols in dust hazardous environments, such as fracking processes, metallic dust compounds, and agriculture dust. The performance of the OPC-N2 is compelling compared to the PAS-1.108 and reference instruments, especially for coarse particles, and may be

suitable for PM<sub>2.5</sub> monitoring after on-site calibration. Despite limitations in the absolute accuracy of the OPC-N2, its low cost and small size offers the ability to assess the temporal-spatial variability of aerosols in various micro-environments. Such data would be useful in identifying the determinants of exposure and the long-term effectiveness of controls put in place to limit those exposures.

## Funding

This research was funded by generous support from NIOSH (R01 OH010533).

## ORCID

Thomas M. Peters  <http://orcid.org/0000-0002-1698-8856>

## References

Alphasense, L. (2015). User Manual: OPC-N2 Optical Particle Counter. 072-0300, Issue 3.

Antonini, J. M. (2003). Health Effects of Welding. *Crit. Rev. Toxicol.*, 33:61–103.

Armendariz, A. J., and Leith, D. (2002). Concentration Measurement and Counting Efficiency for the Aerodynamic Particle Sizer 3320. *J. Aerosol Sci.*, 33:133–148.

Belosi, F., Santachiara, G., and Prodi, F. (2013). Performance Evaluation of Four Commercial Optical Particle Counters. *Atmos. Clim. Sci.*, 03(01):6.

Bhatti, P., Newcomer, L., Onstad, L., Teschke, K., Camp, J., Morgan, M., and Vaughan, T. L. (2011). Wood Dust Exposure and Risk of Lung Cancer. *Occup. Environ. Med.*, 68:599–604.

Brown, J. S., Zeman, K. L., and Bennett, W. D. (2002). Ultrafine Particle Deposition and Clearance in the Healthy and Obstructed Lung. *Am. J. Resp. Crit. Care.*, 166:1240–1247.

Burkart, J., Steiner, G., Reischl, G., Moshammer, H., Neuberger, M., and Hitzenberger, R. (2010). Characterizing the Performance of Two Optical Particle Counters (Grimm OPC1.108 and OPC1.109) Under Urban Aerosol Conditions. *J. Aerosol Sci.*, 41:953–962.

Burnett, R. T., Smith-Doiron, M., Stieb, D., Cakmak, S., and Brook, J. R. (1999). Effects of Particulate and Gaseous Air Pollution on Cardiorespiratory Hospitalizations. *Arch. Environ. Health Int. J.*, 54:130–139.

Cena, L. G., Chisholm, W. P., Keane, M. J., Cumpston, A., and Chen, B. T. (2014). Size Distribution and Estimated Respiratory Deposition of Total Chromium, Hexavalent Chromium, Manganese, and Nickel in Gas Metal Arc Welding Fume Aerosols. *Aerosol. Sci. Technol.*, 48: 1254–1263.

Cheng, Y.-H. (2008). Comparison of the TSI Model 8520 and Grimm Series 1.108 Portable Aerosol Instruments Used to Monitor Particulate Matter in an Iron Foundry. *J. Occup. Environ. Hyg.*, 5:157–168.

Curtis, D. B., Meland, B., Aycibin, M., Arnold, N. P., Grassian, V. H., Young, M. A., and Kleiber, P. D. (2008). A Laboratory Investigation of Light Scattering from Representative Components of Mineral Dust Aerosol at a Wavelength of 550 nm. *J. Geophys. Res. Atmos.*, 113, D08210.

Dockery, D. W., Pope, C. A., Xu, X., Spengler, J. D., Ware, J. H., Fay, M. E., Ferris, B. G., and Speizer, F. E. (1993). An Association between Air Pollution and Mortality in Six U.S. Cities. *New Engl. J. Med.*, 329:1753–1759.

EPA (1997a). 40 CFR Parts 50- Reference Method for the Determination of Fine Particulate Matter as PM<sub>2.5</sub> in the Atmosphere (Appendix L).

EPA (1997b). 40 CFR Parts 50- Reference Method for the Determination of Coarse Particulate Matter as PM<sub>10</sub>–<sub>2.5</sub> in the Atmosphere (Appendix O).

EPA (2006). 40 CFR Parts 53 - General requirements for an equivalent method determination (Subchapter C).

EPA (2016). 40 CFR Parts 58- Ambient Air Quality Surveillance (Subchapter C).

Franck, U., Odeh, S., Wiedensohler, A., Wehner, B., and Herbarth, O. (2011). The Effect of Particle Size on Cardiovascular Disorders — The Smaller the Worse. *Sci. Total Environ.*, 409:4217–4221.

Gao, R., Telg, H., McLaughlin, R., Ciciora, S., Watts, L., Richardson, M., Schwarz, J., Perring, A., Thornberry, T., Rollins, A. (2016). A Light-Weight, High-Sensitivity Particle Spectrometer for PM<sub>2.5</sub> Aerosol Measurements. *Aerosol Sci. Tech.*, 50:88–99.

Giorio, C., Tapparo, A., Scapellato, M. L., Carrieri, M., Apostoli, P., and Bartolucci, G. B. (2013). Field Comparison of a Personal Cascade Impactor Sampler, an Optical Particle Counter and CEN-EU Standard Methods for PM<sub>10</sub>, PM<sub>2.5</sub> and PM<sub>1</sub> Measurement in Urban Environment. *J. Aerosol. Sci.*, 65:111–120.

GRIMM, A. T. G. C. M. (2010). Aerosol spectrometer and dust monitor, series 1.108 and 1.109; M\_E\_IAQ\_1108-1109-Spec\_v2p4.

Grimm, H., and Eatough, D. J. (2009). Aerosol Measurement: The Use of Optical Light Scattering for the Determination of Particulate Size Distribution, and Particulate Mass, Including the Semi-Volatile Fraction. *J. Air Waste Manage Assoc.*, 59:101–107.

Harrison, R. M., Smith, D. J. T., and Kibble, A. J. (2004). What is Responsible for the Carcinogenicity of PM<sub>2.5</sub>? *Occup. Environ. Med.*, 61:799–805.

Hewett, P. (1995). The Particle Size Distribution, Density, and Specific Surface Area of Welding Fumes from SMAW and GMAW Mild and Stainless Steel Consumables. *Am. Ind. Hyg. Assoc.*, 56:128–135.

Hinds, W. C. (1999). *Aerosol Technology: Properties, Behavior, and Measurement of Airborne Particles*, 2nd Ed., New York: Wiley-Interscience.

Järvelä, M., Kauppi, P., Tuomi, T., Luukkonen, R., Lindholm, H., Nieminen, R., Moilanen, E., and Hannu, T. (2013). Inflammatory Response to Acute Exposure to Welding Fumes During the Working Day. *Int. J. Occup. Med. Env. Health*, 26:220–229.

Jean-Baptiste, R., Claire, T., Jean-Luc, M., and Bertrand, G. (2010). Small-Angle Light Scattering by Airborne Particulates: Environnement S.A. Continuous Particulate Monitor. *Meas. Sci. Technol.*, 21:085901.

Kim, S. C., Wang, J., Emery, M. S., Shin, W. G., Mulholland, G. W., and Pui, D. Y. H. (2009). Structural Property Effect of Nanoparticle Agglomerates on Particle Penetration through Fibrous Filter. *Aerosol. Sci. Technol.*, 43:344–355.

Knutson, E. O., and Whitby, K. T. (1975). Aerosol Classification by Electric Mobility: Apparatus, Theory, and Applications. *J. Aerosol. Sci.*, 6:443–451.

Landen, D. D., Wassell, J. T., McWilliams, L., and Patel, A. (2011). Coal Dust Exposure and Mortality from Ischemic Heart Disease Among a Cohort of U.S. Coal Miners. *Am. J. Ind. Med.*, 54:727–733.

Liu, B. Y. H., Berglund, R. N., and Agarwal, J. K. (1974). Experimental Studies of Optical Particle Counters. *Atm. Env.* (1967), 8:717–732.

NIOSH (2012). *Components for Evaluation of Direct-Reading Monitors for Gases and Vapors*. DHHS (NIOSH) Publication No. 2012-162. Cincinnati, OH: National Institute for Occupational Safety and Health.

Ostro, B., Hu, J., Goldberg, D., Reynolds, P., Hertz, A., Bernstein, L., and Kleeman, M. J. (2015). Associations of Mortality with Long-Term Exposures to Fine and Ultrafine Particles, Species and Sources: Results from the California Teachers Study Cohort. *Env. Health Pers.*, 123:549–556.

Parker, J. L., Larson, R. R., Eskelson, E., Wood, E. M., and Veranth, J. M. (2008). Particle Size Distribution and Composition in a Mechanically Ventilated School Building During Air Pollution Episodes. *Indoor Air*, 18:386–393.

Peters, T. M., Ott, D., and O'Shaughnessy, P. T. (2006). Comparison of the Grimm 1.108 and 1.109 Portable Aerosol Spectrometer to the TSI 3321 Aerodynamic Particle Sizer for Dry Particles. *Ann. Occup. Hyg.*, 50:843–850.

Polichetti, G., Cocco, S., Spinali, A., Trimarco, V., and Nunziata, A. (2009). Effects of Particulate Matter (PM10, PM2.5 and PM1) on the Cardiovascular System. *Toxicology*, 261:1–8.

Pope, I. C., Burnett, R. T., and Thun, M. J. (2002). Lung Cancer, Cardiopulmonary Mortality, and Long-Term Exposure to Fine Particulate Air Pollution. *JAMA*, 287:1132–1141.

Samet, J., and Krewski, D. (2007). Health Effects Associated With Exposure to Ambient Air Pollution. *J. Tox. Env. Health A*, 70:227–242.

Schwartz, J., Dockery, D. W., and Neas, L. M. (1996). Is Daily Mortality Associated Specifically with Fine Particles? *J. Air Waste Manage. Assoc.*, 46:927–939.

Schwartz, J., and Neas, L. M. (2000). Fine Particles Are More Strongly Associated than Coarse Particles with Acute Respiratory Health Effects in Schoolchildren. *Epidemiology*, 11:6–10.

Sousan, S., Koehler, K., Thomas, G., Park, J. H., Hillman, M., Halterman, A., and Peters, T. M. (2016). Inter-Comparison of Low-Cost Sensors for Measuring the Mass Concentration of Occupational Aerosols. *Aerosol Sci. Tech.*, 50:462–473.

Syvitski, J. P. (2007). *Principles, Methods and Application of Particle Size Analysis*. Cambridge University Press, Cambridge, UK.

Szymanski, W. W., and Liu, B. Y. H. (1986). On the Sizing Accuracy of Laser Optical Particle Counters. *Part. Part. Syst. Char.*, 3:1–7.

Wang, S. C., and Flagan, R. C. (1990). Scanning Electrical Mobility Spectrometer. *Aerosol Sci. Technol.*, 13:230–240.

Yanosky, J. D., Williams, P. L., and MacIntosh, D. L. (2002). A Comparison of Two Direct-Reading Aerosol Monitors with the Federal Reference Method for PM2.5 in Indoor Air. *Atm. Env.*, 36:107–113.

Zanobetti, A., and Schwartz, J. (2009). The Effect of Fine and Coarse Particulate Air Pollution on Mortality: A National Analysis. *Env. Health Per.*, 117:898–903.